Current Science International Volume : 05 | Issue : 03 | July- Sept. |2016
ISSN: 2077-4435 Pages: 314-324

FT-IR, molecular structure, first order hyperpolarizability, HOMO and LUMO energy gap, NLO and MEP analyses of 4-cyanopyranoquinoline-2-one (CPQ)

[1]El-Mansy M. A. M., [2]M. Ibrahim, [3]H. S. Soliman and [3]S. M. Atef

[1]Molecular Modeling Simulation Lab., Physics Department, Faculty of Education, Ain Shams University, Roxy, Cairo, Egypt.
[2]Spectroscopy Department, National Research Center, 33 El-Bohouth St. 12622, Dokki, Giza, Egypt.
[3]Thin Film Semiconductor Lab., Department of Physics, Faculty of Education, Ain Shams University, Roxy, Cairo, Egypt.

Received: 15 August 2016 / Accepted: 14 Sept. 2016 / Publication date: 25 Sept. 2016

ABSTRACT

A combined experimental and theoretical vibrational study for 4-cyanopyranoquinoline-2-one (CPQ) have been constructed. The optimized molecular structural parameters, vibrational frequencies, thermo-chemical parameters, total dipole moment, nuclear repulsion energy, HOMO-LUMO energy gap, ionization energy, electron affinity, global hardness, electronic chemical potential, global electrophilicity index, softness (ζ) and also first order hyperpolarizability have been investigated for CPQ using DFT/B3LYP utilizing 6-311G(d,p) basis set. Our results showed that CPQ has a high dipole moment (12 Debye) and HOMO-LUMO energy gap of 3.4 eV. Also, CPQ shows a good NLO response which reflects its high applicability as promising Dye Synthesized solar cells (DSSCs). Moreover, we have manipulated the electronic properties of CPQ by applying magnetic field (AMF). CPQ electronic properties enhanced to possess dipole moment (15 Debye) and HOMO/LUMO energy gap (2.3 eV). Manipulation of electronic properties of CPQ by AMF can impact both photovoltaic and spintronic technologies.

Keywords: DFT/B3LYP; FT-IR; HOMO-LUMO energies; AMF/MEP

Introduction

As is well known, various hetero-cyclic compounds are widespread in natural products and attract more attention in many science fields as polymer science, pharmaceutical chemistry (Anizelli *et al.,* 2014; Kumar *et al.,* 2014; Lizarraga *et al.,* 2014; Sert *et al.,* 2014). Also, hetero-cyclic compounds as quinoline-2-one derivatives are characterized by their biological and pharmaceutical activities. Moreover, many quinoline-2-one derivatives are widely used in protein manufacture control, drug synthesis concerning anti-bacterial and anti-fungal activity (El-Nahass *et al.,* 2004). Recently, antitumor drug property has been verified for quinoline-2-one derivatives in chemotherapy (Kılıçoğlu and Ocak, 2011) and excellent reservoir of bioactive substances and valuable intermediates in organic synthesis (Al-Bayati and Radi,2010). Many researchers revealed that quinoline-2-one derivatives are characterized by having high dipole moment and low HOMO-LUMO energy gap, consequently, they are promising structures for photonic devices. For instance, 4-hydroxy-1-methyl-3-[2-nitro-2-oxoacetyl-2(1H)quinolinone (HMNOQ) has a dipole moment of 9 Debye and HOMO–LUMO energy gap of 4 eV that makes it highly recommended to be a promising structure for many applications in optoelectronic devices (Ismail et al., 2013). 4-cyanopyranoquinoline-2-one (CPQ) is the interest of our present study. CPQ is a promising new synthesized organic compound which has a chemical formula of $C_{15}H_9N_3O_5$ as show in Fig. 1 (a). Molecular modeling becomes essential conformational tools used by many authors for confirming their FT-IR experimental spectra (El-Mansy and El-Nahass 2014; El-Mansy and Ismail,2015; El-Mansy and Yahia, 2014). Literature survey reveals that neither quantum chemical calculations nor the vibrational characteristics of CPQ compound have been reported yet. Accordingly, the present investigation was undertaken to study both structural and vibrational characteristics such as optimized molecular structural parameters, vibrational frequencies, thermo-chemical parameters, total dipole moment, nuclear repulsion energy, HOMO-LUMO energy gap, ionization energy (I), electron affinity (A), global hardness (η), electronic chemical potential (μ), global electrophilicity index (ψ), softness (ζ) and also non linear optical (NLO) properties for CPQ using density functional theory (DFT) with Becke–Lee–Yang–Parr (B3LYP) level utilizing 6-311G(d,p) basis set.

Corresponding Author: El-Mansy M. A. M., Molecular Modeling Simulation Lab., Physics Department, Faculty of Education, Ain Shams University, Roxy, Cairo, Egypt.
E-mail: mohamed_mansy878@yahoo.com

Material and methods

Synthesis of CPQ material

Synthesis process for CPQ was proceeded by introducing carbonitrile function at the 4-position of 4-chloro-3-nitropyrano [3, 2-c]quinoline-2,5(6H)-dione under relatively mild conditions. The preparation has been made in two-steps reaction; the first step is converting Cl group to the reactive tosyloxy leaving group at the 4-position via the reaction of 4-chloro-3-nitropyrano [3,2- c]quinoline-2,5(6H)-dione compound with sodium p-toluenesulfonate to give 4-tosylate, and the second to treat the last one with potassium cyanide to give us CPQ Compound (Hassanin, 2012).

FT-IR spectroscopy

CPQ powder (1 mg) was mixed with vacuum dried IR-grad KBr (50 mg) then compressed to a circular disk for performing FT-IR analysis using Thermo Scientific Nicollet 460_{plus} Spectrophotometer at room temperature in the spectral range 500–4000 cm^{-1}.

Theory/Calculation

CPQ vibrational frequencies and IR intensities were calculated using Gaussian 09W program package (Frisch *et al.,* 2009) on a PC Core I5/2.8 GHz using DFT/B3LYP with the extended valence triple-n basis set augmented with polarization functions in both the hydrogen and weighty atoms 6-311G (d,p) basis set without any constraint on the geometry. Gauss View 5 (Frisch *et al.,*2009) was used for visualization of the structure and vibrational frequencies simulation as well. The harmonic vibrational frequencies have been analytically calculated by taking the second order derivative of energy using the same level of theory. The ground state optimized geometry of CPQ molecule is shown in Fig. 1(a). The assignments of the calculated wavenumbers are aided by animation option of Gauss View 5 graphical interface which gives a visual presentation of the shapes of the vibrational modes. Structural parameters corresponding to optimized geometry of CPQ are given in Table 1. The calculated vibrational wavenumbers for CPQ at B3LYP/6-311G(d,p) basis set has been scaled with scaling factor 0.96 for obtaining a considerably better agreement with experimental data (Vijayachamundeeswari *et al.,* 2015)

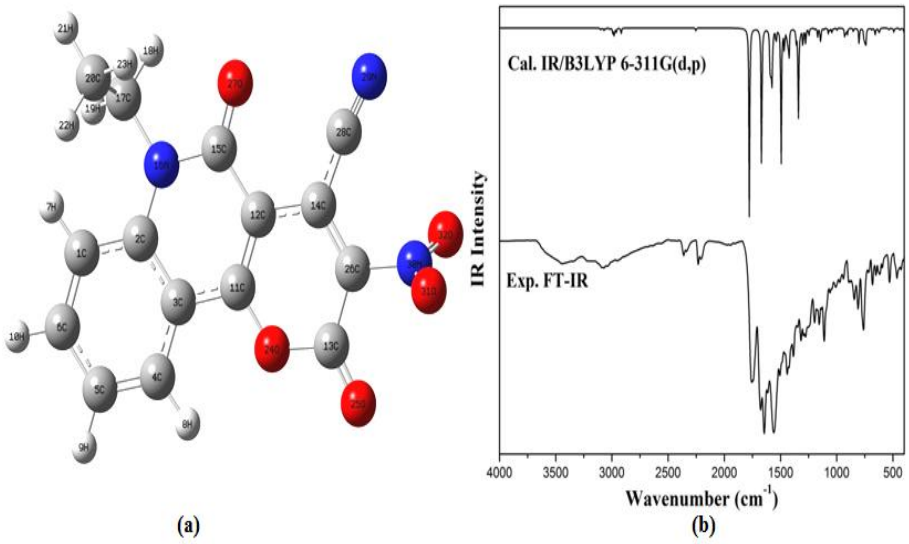

Fig. 1. (a) Optimized molecular structure of CPQ at B3LYP/6-311G(d,p).
(b) Observed and calculated FT-IR spectra for CPQ at B3LYP/6-311G(d,p).

Table 1: Computational Optimized Structural Parameters at B3LYP/6-311G(d,p) for CPQ.

Parameter							
Bond Length (Å)				Bond Angle (°)			
C(1)-C(2)	1.4	C(20)-H(21)	1.1	C(2)-C(1)-C(6)	120.5	C(12)-C(14)-C(26)	118.6
C(1)-C(6)	1.4	C(20)-H(22)	1.1	C(2)-C(1)-H(7)	120.5	C(12)-C(14)-C(28)	122.5
C(1)-H(7)	1.1	C(20)-H(23)	1.1	C(6)-C(1)-H(7)	119.0	C(12)-C(15)-N(16)	116.2
C(2)-C(3)	1.4	C(26)-N(30)	1.5	C(1)-C(2)-C(3)	117.9	C(12)-C(15)-O(27)	122.6
C(2)-N(16)	1.4	C(28)-N(29)	1.2	C(1)-C(2)-N(16)	122.0	N(16)-C(15)-O(27)	121.1
C(3)-C(4)	1.4	N(30)-O(31)	1.2	C(3)-C(2)-N(16)	120.1	C(2)-N(16)-C(15)	123.5
C(3)-C(11)	1.4	N(30)-O(32)	1.2	C(2)-C(3)-C(4)	120.5	C(2)-N(16)-C(17)	121.2
C(4)-C(5)	1.4			C(2)-C(3)-C(11)	117.8	C(15)-N(16)-C(17)	115.3
C(4)-H(8)	1.1			C(4)-C(3)-C(11)	121.7	N(16)-C(17)-H(18)	105.9
C(5)-C(6)	1.4			C(3)-C(4)-C(5)	120.5	N(16)-C(17)-H(19)	108.0
C(5)-H(9)	1.1			C(3)-(4)-H(8)	118.4	N(16)-C(17)-H(20)	113.0
C(6)-H(10)	1.1			C(5)-C(4)-H(8)	121.0	H(18)-C(17)-H(19)	107.8
C(11)-C(12)	1.4			C(4)-C(5)-C(6)	119.2	H(18)-C(17)-C(20)	109.8
C(11)-O(24)	1.3			C(4)-C(5)-H(9)	120.4	H(19)-C(17)-C(20)	112.0
C(12)-C(14)	1.4			C(6)-C(5)-H(9)	120.4	C(17)-C(20)-H(21)	109.7
C(12)-C(15)	1.5			C(1)-C(6)-C(5)	121.4	C(17)-C(20)-H(22)	112.1
C(13)-O(14)	1.4			C(1)-C(6)-H(10)	118.8	C(17)-C(20)-H(23)	110.2
C(13)-O(25)	1.2			C(5)-C(6)-H(10)	119.8	H(21)-C(20)-H(22)	108.2
C(13)-C(26)	1.5			C(3)-C(11)-C(12)	122.1	H(21)-C(20)-H(23)	108.0
C(14)-C(26)	1.4			C(3)-C(11)-O(24)	115.8	H(22)-C(20)-H(23)	108.6
C(14)-C(28)	1.4			C(12)-C(11)-O(24)	122.1	C(11)-O(24)-C(13)	123.8
C(15)-N(16)	1.4			C(11)-C(12)-C(14)	118.3	C(13)-C(26)-C(14)	123.6
C(15)-O(27)	1.2			C(11)-C(12)-C(15)	120.3	C(13)-C(26)-N(30)	114.6
N(16)-C(17)	1.5			C(14)-C(12)-C(15)	121.4	C(14)-C(26)-O(31)	121.9
C(17)-H(18)	1.1			O(24)-C(13)-O(25)	118.5	C(26)-N(30)-O(31)	115.8
C(17)-H(19)	1.1			O(24)-C(13)-C(26)	113.7	C(26)-N(30)-O(32)	117.0
C(17)-C(20)	1.5			O(25)-C(13)-C(26)	127.8	O(31)-N(30)-O(32)	127.2

Results and Discussion

IR spectrum

Experimental and theoretical FT-IR wavenumbers at B3LYP/6-311G(d,p) and the corresponding assignments for CPQ are collected in Table 2. The observed and predicted FT-IR spectra at B3LYP/6-311G(d,p) basis set for CPQ are presented in Fig. 1(b). Our results reveals that predicted vibrational frequencies at B3LYP/6-311G(d,p) give a comparable agreement with the experimental values. The presence of the hydroxyl group (O-H) in a broad band at 3442 cm^{-1} in our observed FT-IR spectrum (cf. Fig. 1(b)) despite the molecular structure of CPQ indicates CPQ is highly affected by atmospheric humidity. The observed discrepancies between experimental (solid phase) and theoretical (gas phase) results are owing to extended hydrogen bonding and stacking interactions, are appropriate. The assignment could be achieved extensively as in the following:

C-H vibrations

The aromatic C-H stretching vibration is observed in the spectral range 3000 – 3100 cm^{-1} (Soliman *et al.,* 2013). The calculated vibration (mode 25) is assigned to aromatic C-H stretching vibrations at 3070 cm^{-1} which is comparable to the experimental value at 3070 cm^{-1}. The calculated vibration (mode 24) is assigned to asymmetric C-H stretching vibration in CH_3 at 2979 cm^{-1} which is commensurate to experimental value at 2930 cm^{-1}. The calculated vibration (mode 23) is assigned to

symmetric C-H stretching vibration in CH_3 at 2918 cm^{-1} which is comparable to experimental value at 2860 cm^{-1}.The C-H in plan bending vibration is observed in the spectral range 1250 – 1280 cm^{-1} (El-Nahass *et al.,* 2013). The calculated vibrations (modes 17, 16, 15, 14) are assigned to C-H in plan bending vibrations at 1248, 1195, 1149, 1143 cm^{-1} which are commensurate to experimental values at 1277, 1197, 1156, 1135 cm^{-1}.The C-H out of plan bending vibration is observed in the spectral range 690 – 850 cm^{-1} (El-Mansy *et al.,* 2013). The calculated vibrations (modes 9, 8, 7) are assigned to C-H out of plan bending vibrations at 840, 802 and 743 cm^{-1} which are comparable to our experimental values at 844, 810 and 762 cm^{-1}.

Table 2: Experimental and Computational Calculated Vibrational Wavenumbers (Harmonic Frequency (cm^{-1})), IR Intensities, Species and Assignments for CPQ at B3LYP/6-311G(d,p).

No	Exp.	B3LYP/6-311G (d,p)				Species	Vibrational Assignment
		Wave number		IR intensity			
		Unscaled	Scaled	Rel.	Abs.		
1	428	455	437	3	1	A"	
2	464	458	440	4	1	A"	γC-C + γC-O + γC-N
3	530	563	540	4	1	A"	
4	617	646	620	11	2	A'	
5	650	687	659	20	3	A'	βC-C + βC-O + βC-N
6	682	718	689	6	1	A'	
7	762	773	743	75	13	A"	
8	810	835	802	52	9	A"	γC-H
9	844	875	840	1	0	A"	
10	940	956	918	10	2	A'	υC-C
11	973	1041	999	7	1	A'	υC-N
12	1009	1086	1042	16	3	A'	υC-O
13	1112	1161	1114	4	1	A'	
14	1135	1190	1143	47	8	A'	
15	1156	1197	1149	5	1	A'	βC-H
16	1197	1244	1195	3	0	A'	
17	1277	1300	1248	26	4	A'	
18	1440	1508	1448	10	2	A'	CH_3deformation
19	1560	1633	1567	25	4	A'	υC=C
20	1600	1643	1578	231	39	A'	υN=O
21	1677	1851	1777	586	100	A'	υC=O
22	2232	2347	2254	9	2	A'	υC≡N
23	2860	3040	2918	17	3	A'	υ_s C-H in CH_3
24	2930	3103	2979	25	4	A'	υ_{as}C-H in CH_3
25	3070	3197	3070	7	1	A'	υC-H (aromatic)

υ (stretching); β (in plane bending); γ (out of plane bending); A'(in-plane & stretching); A"(out-of-plane)

C≡N vibrations

The C≡N stretching vibration is observed in the spectral range 2300 – 2100 cm^{-1} (Ibrahim *et al.,* 2013). The calculated vibration (mode 22) is assigned to C≡N stretching vibration at 2254 cm^{-1} which is comparable to the experimental value at 2232 cm^{-1}.

C=O, C=C vibrations

The C=O stretching vibration is observed in the spectral range 1790 – 1670 cm^{-1} (Karthikeyan *et al.,* 2015). The calculated vibration (mode 21) is assigned to C=O stretching vibration at 1669 cm^{-1} which is comparable to experimental value at 1677 cm^{-1}.The calculated vibration (mode 20) is assigned to N=O stretching vibration at 1578 cm^{-1} which is comparable to experimental value at 1614 cm^{-1}. The C=C stretching vibration is observed in the spectral range 1480 – 1630 cm^{-1} (El-Barbary *et al.,* 2009). The calculated vibrations (mode 19) is assigned to C=C stretching vibration at1567 cm^{-1} which is comparable to experimental value at 1560 cm^{-1}.

Methyl group vibrations

The CH_3 deformation is observed in the spectral range 1410 - 1450 cm^{-1} (Soliman *et al.,* 2012). The calculated vibration (mode 18) is assigned to CH_3 deformation at 1448 cm^{-1} which is commensurate to experimental value at 1440 cm^{-1}.

C-O, C-N, C-C vibrations

The calculated vibration (mode 12) is devoted to C-O stretching vibration at 1042 cm^{-1} which is comparable to experimental value at 1009 cm^{-1}. The calculated vibration (mode 11) is assigned to C-N stretching vibration at 999 cm^{-1} which is commensurate to experimental value at 973 cm^{-1}. The calculated vibration (mode 10) is assigned to C-C stretching vibration at 918 cm^{-1} which is comparable to experimental value at 940 cm^{-1}.The calculated vibrations (modes 6, 5, 4) are assigned to C-C, C-O and C-N in plane vibrations at 689, 659, 620 cm^{-1} which are comparable to the experimental values at 682, 650, 617 cm^{-1}. The calculated vibrations (mode 3, 2, 1) are assigned to C-C, C-O and C-N out of plane vibrations at 540, 440 and 437 cm^{-1} which are commensurate to the experimental values at 530, 464 and 428 cm^{-1}.

Thermochemistry

Thermochemistry is the science concerning with the energy or heat associated with chemical reactions and/or physical transformations for a molecular system. Also, it is mainly focused on energy changes, particularly on the system's energy exchange with its surroundings. Thermochemistry combines the concepts of both thermodynamics and chemical bonds energies. Such combination includes calculations of various quantities as heat capacity, heat of combustion, heat of formation, enthalpy, entropy, free energy. In our current study, many calculated thermo-chemical parameters for CPQ at B3LYP/6-311G(d,p) such as total energy, zero-point vibrational energy, rotational constants, entropy (S) and specific heat (C_V) at room temperature are tabulated in Table 3.

Table 3: The Optimized Calculations of Total Energies (a.u), Zero Point Vibrational Energies (kcal mol^{-1}), Rotational Constants (GHz), Entropies(cal k^{-1}), Molar Specific Heat C_V(cal k^{-1}), Total Dipole Moment (Debye), Nuclear Repulsion Energy (eV), E_{LUMO} and E_{HOMO}(eV), HOMO-LUMO Energy Gap (eV), Ionization Energy (I) (eV), Electron Affinity (A) (eV),Global Hardness (η) (eV), Electronic Chemical Potential (μ) (eV), Global Electrophilicity Index (ψ) (eV) and finally softness (ζ) (eV^{-1}) for CPQ at B3LYP/6-311G(d,p).

Parameter	B3LYP/6-311G (d,p)
Total Energy	-1117.5638464
Zero Point Energy	140.17604
Rotational Constants	0.45907 0.19916 0.14348
Entropy	
Total	143.4
Transational	43.1
Vibrational	65.8
Rotational	34.5
Nuclear Repulsion Energy	5.1×10^4
Molar Specific Heat C_v	71
Dipole Moment	11
E_{LUMO}	-3.67
E_{HOMO}	-7.1
HOMO-LUMO energy gap	3.4
Ionization energy (I)	7.1
Electron Affinity (A)	3.7
Global Hardness (η)	1.7
Chemical Potential (μ)	5.4
Global Electrophilicity Index (ψ)	8.6
Softness (ζ)	0.6

According to the molecular orbital theory, the ionization energy (I) (the minimum amount of energy required to remove an electron (to infinity) from the atom or molecule in the gaseous state) and electron affinity (A) (the amount of energy released when an electron is added to a neutral atom or molecule in the gaseous state to form a negative ion) can be expressed by HOMO and LUMO orbital energies as $I = -E_{HOMO}$ and $A = -E_{LUMO}$. The global hardness (Resistance towards the deformation of electron cloud or polarization of chemical systems under small perturbation encountered during chemical processes) is given by $\eta = 1/2(E_{LUMO} - E_{HOMO})$. The electron affinity can be used in combination with ionization energy to give electronic chemical potential (the amount of absorbed or released potential energy during a chemical reaction), $\mu = 1/2(E_{LUMO} + E_{HOMO})$. The global electrophilicity index (the molecule ability to donate

electrons), $\psi = \mu^2 /2\eta$ and softness (the reciprocal of global hardness), $\zeta = 1/\eta$(Soliman *et al.,* 2012). These parameters have been evaluated and tabulated in Table 3.

Frontier molecular orbitals and its related physical parameters

Frontier molecular orbitals are very important in molecular modeling. The highest occupied molecular orbitals (HOMOs) and lowest unoccupied molecular orbitals (LUMOs) reflect the chemical activity of the studied molecule. Since HOMO is a measure of the ease of electron loss and LUMO is a measure of the ease of electron gain. Therefore, HOMO/LUMO molecular orbitals are considered as an accurate indicator for electron transport chargeability in molecular systems (Sheela *et al.,* 2015). CPQ possesses a dipole moment (12 Debye) and HOMO/LUMO energy gap of 3.4 eV which indicates its high reactivity to interact with the surrounding media and extended applicability for manufactured photovoltaic devices such as solar cells. Figure 2(a) shows the calculated HOMO-LUMO molecular orbitals of CPQ at B3LYP/6-311G(d,p). Figure 2(b) presents the calculated density of state (DOS) spectrum for CPQ at B3LYP/6-311G(d,p). The total DOS spectrum was scaled by 0.5. It is noted that the HOMOs of CPQ are π orbitals while the LUMOs are π* orbitals.

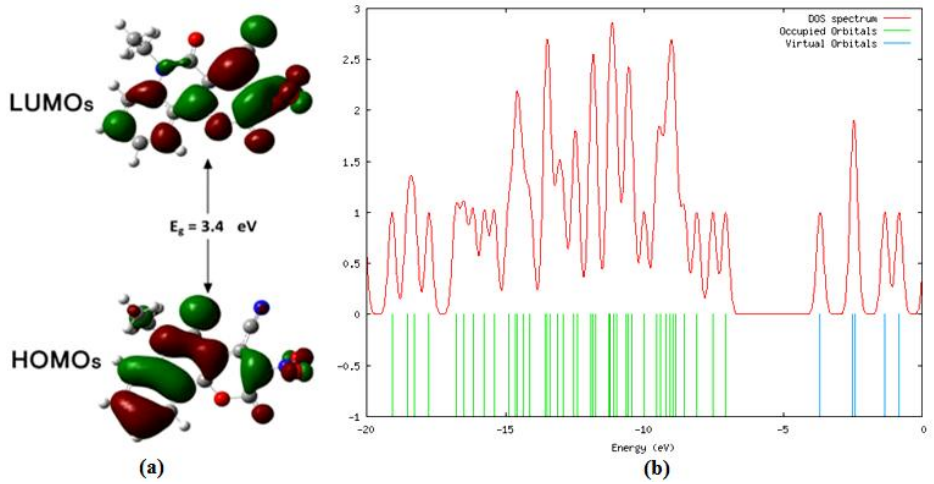

Fig. 2. (a) LUMO-HOMO Energy Gap for CPQ at B3LYP/6-311G(d,p).
(b) Density of state (DOS) spectrum for CPQ at B3LYP/6-311G(d,p).

Polarizability and first order hyperpolarizability calculations

In order to investigate the relationships among molecular structures and non-linear optical properties (NLO), the polarizabilities and first order hyperpolarizabilities of CPQ compound was calculated using B3LYP/6-311G(d,p) basis set, based on the finite-field approach. The polarizability and hyperpolarizability tensors (α_{xx}, α_{xy}, α_{yy}, α_{xz}, α_{yz}, α_{zz} and β_{xxx}, β_{xxy}, β_{xyy}, β_{yyy}, β_{xxz}, β_{xyz}, β_{yyz}, β_{xzz}, β_{yzz}, β_{zzz}) are obtained by a frequency job output Gaussian file. The mean polarizability (α_{tot}), anisotropy of polarizability ($\Delta\alpha$) and the average value of the first order hyperpolarizabiliy (β_{tot}) can be calculated using the equations (Akhtari *et al.,* 2014):

$$\alpha_{tot} = \frac{\alpha_{xx} + \alpha_{yy} + \alpha_{zz}}{3}$$

$$\Delta\alpha = \frac{1}{\sqrt{2}}\left[(\alpha_{xx} - \alpha_{yy})^2 + (\alpha_{yy} - \alpha_{zz})^2 + (\alpha_{zz} - \alpha_{xx})^2 + 6\alpha_{yz}^2 + 6\alpha_{xy}^2 + 6\alpha_{xz}^2\right]^{1/2}$$

$$\beta_{tot} = \left[(\beta_{xxx} + \beta_{xyy} + \beta_{xzz})^2 + (\beta_{yyy} + \beta_{yzz} + \beta_{yxx})^2 + (\beta_{zzz} + \beta_{zxx} + \beta_{zyy})^2\right]^{1/2}$$

The higher values of dipole moment, molecular polarizability and first order hyperpolarizability are important indicator of highly active NLO properties of CPQ. Believing this we may expect the usage of the compound under investigation in non-linear devices. The first order hyperpolarizability (β_{tot}) and the components of hyperpolarizability β_x, β_y and β_z of CPQ along with related properties ($\Delta\alpha$ *and* α_{tot}) are reported in Table 4. The calculated values have been converted into electronic units (esu)) (α; 1 a.u. = 0.1482×10^{-24} esu, β; 1 a.u. = 8.6393×10^{-33} esu) . The calculated polarizability and anisotropy of the polarizability of CPQ are 31.58 x 10^{-24} and 27.04 x 10^{-24} esu, respectively. The magnitude of the molecular hyperpolarizability (β) is one of important key factors in a NLO system. The calculated first order hyperpolarizability value (β_{tot}) of CPQ is equal to 7.36 x 10^{-30} esu which is 19 times higher than urea (β_{urea} = 0.3728 x10^{-30} esu) (Vijayachamundeeswari *et al.,* 2015). CPQ is a promising material for optoelectronic device applications as it shows a good NLO response.

Table 4 :Mean polarizability α_{tot} (x10^{-24} esu), anisotropy polarizability $\Delta\alpha$ (x10^{-24} esu) and first order hyperpolarizability β_{tot} (x10^{-30} esu) for CPQ based on B3LYP/6-311G(d,p) basis set.

Parameters	Values	Parameter	Value
α_{xx}	44.65	β_{xxx}	10.75
α_{xy}	2.53	β_{xxy}	1.51
α_{yy}	35.45	β_{xyy}	-2.89
α_{xz}	0.30	β_{yyy}	-2.65
α_{yz}	-0.95	β_{xxz}	0.04
α_{zz}	14.64	β_{xyz}	0.17
α_{tot}	31.58	β_{yyz}	-0.02
$\Delta\alpha$	27.04	β_{xzz}	-0.58
		β_{yzz}	0.09
		β_{zzz}	0.00
		β_{tot}	7.36

Manipulating magnetic field effects on CPQ

Applying an external magnetic field (AMF) on CPQ may have many remarkable changes in its physical and chemical properties according to its high dipole moment value (12 Debye). Our computations have been based on the idea that AMF will affect the electron clouds to be deformed and electron spin will be aligned in the direction of magnetic field, which raises the probability for nitrogen dioxide group (NO_2) to interact with adjacent cyano (C≡N) group to form a metastable state as presented in Fig. 3. After removing AMF, we speculate that there are two probabilities that may exist, either CPQ retains its original structure or turns into new structure in which cyano group captured an oxygen atom from adjacent nitrogen dioxide group. Such probability has remarkable changes in the physical and chemical properties of CPQ. The partial charges on N(29) and N(30) atoms changed from -0.180, 0.022 to -0.165 and -0.027a.u (cf. Table 4), respectively. Moreover, The partial charges on O(31) and O(32) atoms changed from -0.168, -0.35 to -0.225 and -0.225a.u, respectively. Alternatively, the partial charges on C(14), C(26) and C(28) atoms changed from -0.106, -0.157,0.345 to 0.285, -0.027and 0.082 a.u, respectively. Partial charges variations induce an appropriate effect in both dipole moment value (15 Debye) and the HOMO/LUMO energy gap (2.3 eV) (cf. Fig. 3). Change in HOMO-LUMO Energy Gap (eV), Dipole Moment (Debye) and Partial charges for CPQ due to AMF at B3LYP/6-311G(d,p) are reported in Table 5. Manipulation of electronic properties of CPQ by magnetic field could have a high impact on the electronic and spintronic technologies (Chikazumi, and Graham, 1997; Cullity and Graham,2011). This can be achieved by affecting the functionality of various organic-based devices such as light-emitting diodes, photovoltaics, and field-effect transistors, and by enabling the invention of novel spintronic devices such as flexible memory storage(Blundell and Pratt,2004).

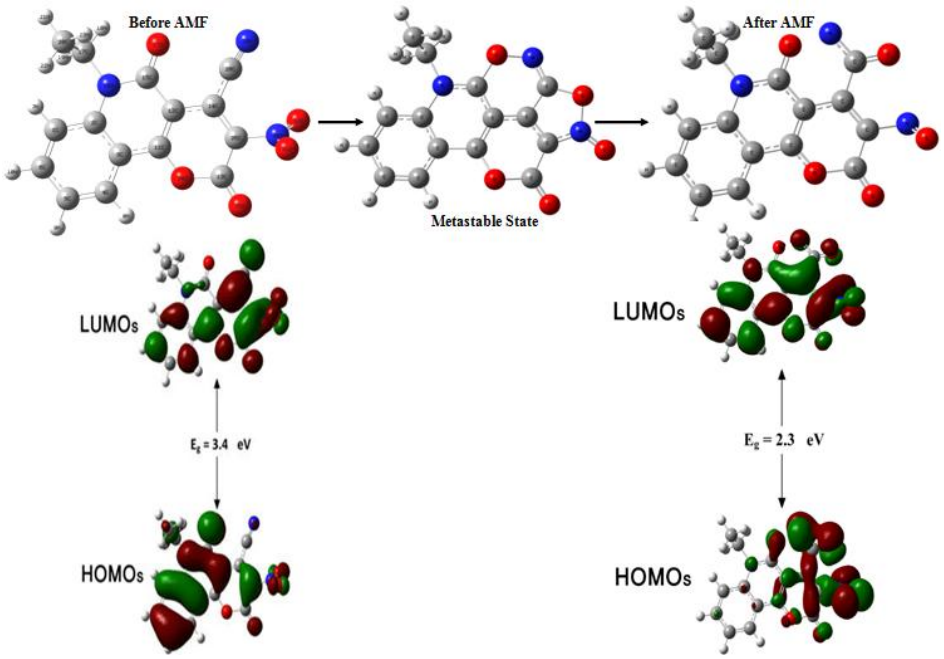

Fig. 3. Manipulating magnetic field effects on CPQ at B3LYP/6-311G(d,p).

Table 5: Change in HOMO-LUMO Energy Gap (eV), Dipole Moment (Debye) and Partial charges for CPQ due to AMF at B3LYP/6-311G(d,p).

	B3lYP/6-311G(d,p)	
	Before AMF	After AMF
HOMO-LUMO energy gap	3.4	2.3
Dipole Moment	12	15
Partial Charges		
C(26)	-0.157	-0.027
N(30)	0.022	0.161
O(31)	-0.168	-0.225
C(14)	0.106	0.285
C(28)	0.345	0.082
O(32)	-0.351	-0.225
N(29)	-0.180	-0.165

Molecular electrostatic potential surface analysis

Molecular electrostatic potential (MEP) is a 3D plot of electrostatic potential mapping over the whole constant electron density surface. MEP presents molecular size, shape and electrostatic potential values. Electrostatic potential physically correlates with many other physical properties of molecular structure such as dipole moment, electronegativity, partial charges and molecular chemical reactivity sites of the investigated molecule. MEP provides a visual map for the relative polarity of a molecule (Şahin *et al.,* 2015). The positive electrostatic potential corresponds to repulsion of the proton by the atomic nuclei in regions where low electron density exists and the nuclear charge is incompletely shielded. The negative electrostatic potential corresponds to attraction of the proton by the atomic nuclei in regions where high electron density exists and the nuclear charge is completely shielded. The electrostatic potential values are represented by different colors. The positive, negative and neutral electrostatic potential regions of molecules are shown in terms of color grading. Potential increases in the order red < orange < yellow < green< blue. Generally the red color indicates the maximum negative region and the blue color represents the maximum positive region. The region of intermediary potential is explored by yellow and green colors. The regions of extreme potentialsappear at red and blue colors are the key indicators of electronegativity. MEP is mapped up at the level of B3LYP/6-311G(d,p) theory with optimized geometry for CPQ before and after AMF as shown in Fig. 4 (a&b). As can be seen from the MEP map of the title molecule, the negative regions are mainly localized on both oxygen atom carbonyl (C=O) groups and nitrogen atom of cyano (C≡N) group which indicating possible sites for electrophilic attacks. Whereas, the maximum

positive region which localized over the H atoms of phenyl ring indicating possible sites for nucleophilic attacks.

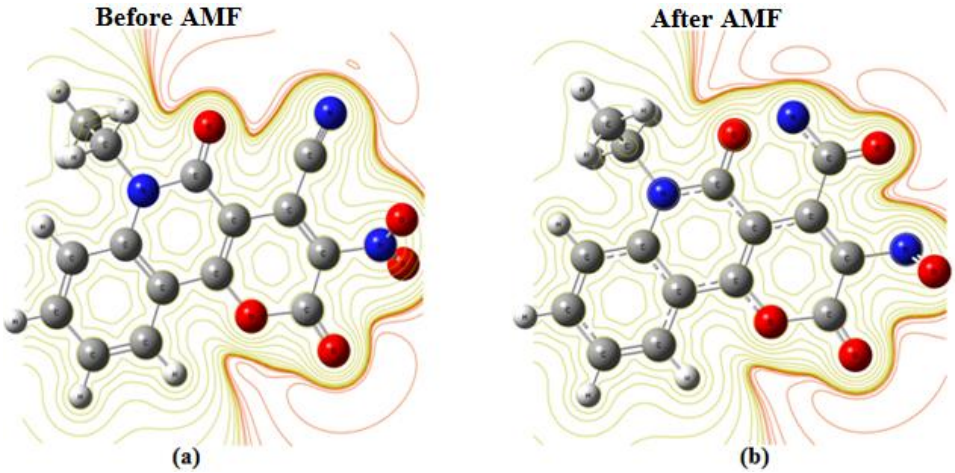

Fig. 4. MEP mapping for CPQ (a)Before and (b) after AMF using B3LYP/6-311G(d,p).

Conclusion

CPQ has a high dipole moment (12 Debye), HOMO-LUMO energy gap of 3.4 eV and shows a good NLO response which reflects its high applicability for many applications in optoelectronic devices. Physical properties of CPQ are enhanced by AMF in which dipole moment value increased up to15 Debye and HOMO/LUMO energy gap is decreased down to 2.3 eV. Manipulation of electronic properties of CPQ by magnetic field can impact both electronic and spintronic technologies– by affecting the functionality of various organic-based devices such as light-emitting diodes, photovoltaics, and field-effect transistors, and by enabling the invention of novel spintronic devices such as flexible memory storage. Any discrepancies noted between calculated and experimental vibrational frequencies may be due to the fact that the calculations have been actually performed on a single molecule in the gaseous state contrary to the experimental values that recorded in the presence of intermolecular interactions.

References

Akhtari, K. K. Hassanzadeh, B. Fakhraei, H. Hassanzadeh, G. Akhtari, S.A. Zarei,2014. First hyperpolarizability orientation in [70] PCBM isomers: A DFT study, Computational and Theoretical Chemistry, 1038 : 1-5.

Al-Bayati, R.I., M.F. Radi, 2010.Synthesis of novel 2-quinolone derivatives, Afr J Pure Appl Chem, 4 : 228-232.

Anizelli, P.R., J.P. Baú, H.S. Nabeshima, M.F. da Costa, H. de Santana, D.A. Zaia, 2014. An experimental and theoretical vibrational study of interaction of adenine and thymine with artificial seawaters: A prebiotic chemistry experiment, Spectrochimica Acta Part A: Molecular and Biomolecular Spectroscopy, 126 : 184-196.

Blundell, S.J. and F.L. Pratt,2004. Organic and molecular magnets, Journal of Physics: Condensed Matter, 16 : R771.

Chikazumi, S. and C. Graham,1997. Physics of Ferromagnetism (International Series of Monographs on Physics), in, Oxford University Press, New York.

Cullity B.D. and C.D. Graham,2011. Introduction to magnetic materials, John Wiley & Sons, 2011.

El-Barbary, A.A., M.M. El-Nahass, M.A. Kamel, M.A.M. El-Mansy,2009. FT-IR, FT-Raman Spectra and Ab Initio HF, DFT Vibrational analysis of P-methyl acetanilide, Journal of Applied Sciences Research 11 : 1977-1987.

El-Mansy, M. and M. El-Nahass, 2014. On the spectroscopic analyses of Perylene-66, Spectrochimica Acta Part A: Molecular and Biomolecular Spectroscopy, 130 : 568-573.

El-Mansy, M., M. El-Nahass, N. Khusayfan, E. El-Menyawy,2013. DFT approach for FT-IR spectra and HOMO–LUMO energy gap for N-(p-dimethylaminobenzylidene)-p-nitroaniline (DBN), Spectrochimica Acta Part A: Molecular and Biomolecular Spectroscopy, 111 : 217-222.

El-Mansy, M., M. Ismail, 2015.On the spectroscopic analyses of 3-(4-Hydroxy-1-methyl-2-oxo-1, 2-dihydro-quinolin-3-yl)-2-nitro-3-oxo-propionic acid (HMQNP), Spectrochimica Acta Part A: Molecular and Biomolecular Spectroscopy, 135 : 704-709.

El-Mansy,M. and I. Yahia, 2014. Spectroscopic notes of Methyl Red (MR) dye, Spectrochimica Acta Part A: Molecular and Biomolecular Spectroscopy, 130 :59-63.

El-Nahass, M., H. Zeyada, M. Aziz, N. El-Ghamaz, 2004. Structural and optical properties of thermally evaporated zinc phthalocyanine thin films, Optical Materials, 27 : 491-498.

El-Nahass, M., M. Kamel, A. El-Barbary, M. El-Mansy, M. Ibrahim, 2013. FT-IR spectroscopic analyses of 3-Methyl-5-Pyrazolone (MP), Spectrochimica Acta Part A: Molecular and Biomolecular Spectroscopy, 111 : 37-41.

Frisch, A., R. Dennington, T. Keith, J. Millam, A. Nielsen, A. Holder, J. Hiscocks,2009. Gauss view version 5 user manual, Gaussian Inc., Wallingford, CT, USA.

Frisch, G.W.T. M. J., H. B. Schlegel, G. E. Scuseria, M. A. Robb, J. R. Cheeseman, J. A. Montgomery, Jr., T. Vreven, K. N. Kudin, J.C. Burant, J. M. Millam, S.S. Iyengar, J. Tomasi, V. Barone, B. Mennucci, M. Cossi, G. Scalmani, N. Rega, G. A. Petersson, H. Nakatsuji, M. Hada, M.Ehara, K. Toyota, R. Fukuda, J. Hasegawa, M. Ishida, T. Nakajima, Y. Honda, O. Kitao, H. Nakai, M. Klene, X. Li, J. E. Knox, H.P. Hratchian, J.B. Cross, C. Adamo, J. Jaramillo, R. Gomperts, R. E. Stratmann, O. Yazyev, A.J. Austin, R.Cammi, C. Pomelli, J.W. Ochterski, P.Y. Ayala, K. Morokuma, G.A. Voth, P. Salvador, J. J. Dannenberg, V.G. Zakrzewski, S. Dapprich, A.D. Daniels, M.C. Strain, O. Farkas, D.K. Malick, A.D. Rabuck, K. Raghavachari, J. B. Foresman, J. V. Ortiz, Q. Cui, A.G. Baboul, S. Clifford, J. Cioslowski, B. B. Stefanov, G. Liu, A. Liashenko, P. Piskorz, I. Komaromi, R.L. Martin, D.J.Fox, T. Keith, M. A. Al-Laham, C.Y. Peng, A. Nanayakkara, M. Challacombe, P. M. W. Gill, B. Johnson, W. Chen, M. W. Wong, C. Gonzalez, J. A. Pople, Gaussian09, Revision A, Inc., Wallingford CT, (2009).

Hassanin, H.M., 2012. Nucleophilic Substitution and Ring Transformation Reactions with 4-Chloro-6-ethyl-3-nitropyrano [3, 2-c] quinoline-2, 5-(6H)-diones, Arkivoc, 6 : 384-397.

Ibrahim, M., M. El-Nahass, M. Kamel, A. El-Barbary, B. Wagner, M. El-Mansy, 2013. On the spectroscopic analyses of thioindigo dye, Spectrochimica Acta Part A: Molecular and Biomolecular Spectroscopy, 113 : 332-336.

Ismail, M., G. Morsy, H. Mohamed, M. El-Mansy, M. Abd-Alrazk, 2013. FT-IR spectroscopic analyses of 4-hydroxy-1-methyl-3-[2-nitro-2-oxoacetyl-2 (1H) quinolinone (HMNOQ), Spectrochimica Acta Part A: Molecular and Biomolecular Spectroscopy, 113 : 191-195.

Karthikeyan, N., J.J. Prince, S. Ramalingam, S. Periandy,2015. Spectroscopic [FT-IR and FT-Raman] and theoretical [UV–Visible and NMR] analysis on α-Methylstyrene by DFT calculations, Spectrochimica Acta Part A: Molecular and Biomolecular Spectroscopy, 143 : 107-119.

Kılıçoğlu, T., Y.S. Ocak,2011. Electrical and photovoltaic properties of an organic–inorganic heterojunction based on a BODIPY dye, Microelectronic Engineering, 88 :150-154.

Kumar, C.C., C.Y. Panicker, H.-K. Fun, Y.S. Mary, B. Harikumar, S. Chandraju, C.K. Quah, C.W. Ooi, 2014. FT-IR, molecular structure, first order hyperpolarizability, HOMO and LUMO analysis, MEP and NBO analysis of 2-(4-chlorophenyl)-2-oxoethyl 3-nitrobenzoate, Spectrochimica Acta Part A: Molecular and Biomolecular Spectroscopy, 126 : 208-219.

Lizarraga, E., D.M. Gil, G.A. Echeverría, O.E. Piro, C.A. Catalán, A.B. Altabef,2014. Synthesis, crystal structure, conformational and vibrational properties of 6-acetyl-2, 2-dimethyl-chromane, Spectrochimica Acta Part A: Molecular and Biomolecular Spectroscopy, 127 : 74-84.

Şahin, Z.S., H. Şenöz, H. Tezcan, O. Büyükgüngör,2015. Synthesis, spectral analysis, structural elucidation and quantum chemical studies of (E)-methyl-4-[(2-phenylhydrazono) methyl] benzoate, Spectrochimica Acta Part A: Molecular and Biomolecular Spectroscopy, 143 : 91-100.

Sert, Y., S. Sreenivasa, H. Doğan, K. Manojkumar, P. Suchetan, F. Ucun,2014. FT-IR, Laser-Raman spectra and quantum chemical calculations of methyl 4-(trifluoromethyl)-1H-pyrrole-3-carboxylate-A DFT approach, Spectrochimica Acta Part A: Molecular and Biomolecular Spectroscopy, 127 : 122-130.

Sheela, G.E., D. Manimaran, I.H. Joe, S. Rahim, V.B. Jothy,2015. Structure and nonlinear optical property analysis of l-Methioninium Oxalate: A DFT approach, Spectrochimica Acta Part A: Molecular and Biomolecular Spectroscopy, 143 : 40-48.

Soliman, H., K.M. Eid, H. Ali, M. El-Mansy, S. Atef,2013. FT-IR spectroscopic analyses of 2-(2-furanylmethylene) propanedinitrile, Spectrochimica Acta Part A: Molecular and Biomolecular Spectroscopy, 105 (2013) 545-549.

Soliman, H., K.M. Eid, H. Ali, S. Atef, M. El-Mansy,2012. Vibrational spectroscopic analysis of 2-chloro-5-(2, 5-dimethoxy-benzylidene)-1, 3-diethyl-dihydro-pyrimidine-4, 6 (1H, 5H)-dione, Spectrochimica Acta Part A: Molecular and Biomolecular Spectroscopy, 97 : 1079-1084.

Vijayachamundeeswari, S., B.Y. Narayana, S.J. Pradeepa, N. Sundaraganesan, 2015. Vibrational analysis, NBO analysis, NMR, UV–VIS, hyperpolarizability analysis of Trimethadione by density functional theory, Journal of Molecular Structure, 1099 : 633-643.